



Machining characteristics of fine grained AZ91 Mg alloy processed by friction stir processing

G. V. V. SURYA KIRAN¹, K. HARI KRISHNA¹, Sk. SAMEER¹, M. BHARGAVI¹, B. SANTOSH KUMAR¹,
G. MOHANA RAO¹, Y. NAIDUBABU¹, RAVIKUMAR DUMPALA², B. RATNA SUNIL¹

1. Department of Mechanical Engineering,

Rajiv Gandhi University of Knowledge Technologies (AP-IIIT), Nuzvid 521202, India;

2. Department of Mechanical Engineering,

Visvesvaraya National Institute of Technology, Nagpur 440010, India

Received 7 April 2016; accepted 29 October 2016

Abstract: AZ91 Mg alloy was considered and friction stir processing (FSP) was adopted to achieve grain refinement to investigate the effect of grain size and secondary phase on machining characteristics during drilling at various speeds and feeds. Super saturated AZ91 Mg alloy was obtained after FSP and the grain refinement was achieved from $(166.5 \pm 8.7) \mu\text{m}$ to $(21.7 \pm 13.5) \mu\text{m}$. Surprisingly, hardness reduced for FSP AZ91 Mg alloy (88.95 ± 6.1) compared with AZ91 alloy (108.2 ± 15.6), which was attributed to the reduced secondary phase. However, the mean cutting force for FSP-treated (FSPed) AZ91 Mg alloy was marginally increased. The edge damage of the drilled holes was lower for FSPed AZ91 Mg alloy compared with unprocessed AZ91 Mg alloy. Hence, it can be understood that the grain refinement may slightly increase the cutting forces during drilling but better edge finishing can be achieved in machining of AZ91 Mg alloy.

Key words: magnesium alloy; friction stir processing; machining; grain size; microstructure

1 Introduction

Interest towards light metals as structural components is tremendously being increased in the modern manufacturing industry with an objective to develop energy efficient structures. Therefore, magnesium and its alloys have become alternate choice apart from the aluminum and its alloys. Magnesium has lower density compared with aluminum and higher specific strength compared with other available metallic systems [1,2]. On the other hand, microstructural modification to improve the mechanical and tribological behavior of metals is well accepted strategy in the materials research field. Modifying the microstructure of metal has also shown significant effects on altering different structure sensitive properties. Recently, many processing techniques were developed to produce fine grained structures. Friction stir processing is one of such advanced techniques that can be used to modify the microstructure without melting the metal [3].

Machining of material is one of the basic

manufacturing processes usually found in developing structures and components in the manufacturing industry [4]. The grain refined metals which exhibit improved mechanical properties also must be machined in order to produce components for different structural applications. Recently, LAPOVOK et al [5] studied the machining characteristics of ultra fine grained commercial pure titanium (CP-Ti) and demonstrated that the overall machining properties were better for grain refined CP-Ti compared with coarse grained CP-Ti.

Machining of Mg alloys is slightly complex due to the inflammable nature and formation of flank built-up (FBU) at higher cutting speeds [1,6]. It was reported that the chip temperature is increased with higher cutting speeds during turning of AZ31 alloy [7,8]. AKYUZ [9] have studied the machining characteristics of AZ series alloys during turning and reported that AZ91 showed lower cutting forces compared with AZ21 alloy. Very recently, we have observed a significant effect of aluminium content on machining during drilling of AZ series Mg alloys [10]. However, the information on the machining behavior of fine grained metals is limited in

the literature, particularly lacking for fine grained Mg alloys. Therefore, in the present study, AZ91 Mg alloy was selected and grain refinement was achieved by friction stir processing (FSP). The effect of microstructural modification on machining characteristics was investigated during drilling.

2 Experimental

AZ91 Mg alloy (8.67% Al, 0.85% Zn, 0.002% Fe, 0.03% Mn and balance Mg in mass fraction) cast sheets were obtained from Exclusive Magnesium, Hyderabad, India. FSP was done using an automated universal milling machine (Bharat Fritz Werner Ltd., India). FSP tool was made of H13 tool steel with a shoulder diameter of 15 mm. FSP tool has a tapered pin of 3 mm in length with 3 mm to 1 mm taper. Optimized process parameters (1400 r/min tool rotational speed and 25 mm/min feed) were obtained after a few trial experiments. A penetration depth of 3 mm was given such a way that the tool shoulder touched the work piece surface. Then, the rotating FSP tool was plunged across the length as shown in Fig. 1(a). The processed AZ91 Mg alloy was coded as FSPed AZ91.

The received AZ91 Mg alloy was characterized by X-ray powder diffraction (XRD) method with Cu K_{α} radiation (step size 0.1°). Microstructural observations were carried out for unprocessed AZ91 Mg alloy (coded as AZ91) and FSPed AZ91. The samples were metallographically polished and chemical etching was done by picric acid reagent (comprised of 5 g picric acid, 5 mL acetic acid, 5 mL distilled water and 100 mL ethanol). Then, the samples were rinsed with ethanol and dried in hot air. Microstructural observations were carried out using a polarized optical microscope (Leica, Germany) at different regions of the samples. Microhardness measurements were carried out by Vickers indentation method (Omnitech, India) by applying 100 g load for 10 s.

Machining experiments were conducted on a vertical milling machine using 6 mm-diameter twist drill bit made of high speed steel. Initially, the work piece was fixed on a dynamometer (Kistler, Switzerland) and the entire set up was fixed on the work table of the milling machine as shown in Fig. 1(b). Drilling was carried out at different tool rotational speeds (90, 180 and 355 r/min) and at different feed rates (16, 20 and 25 mm/min). Holes were produced on both the work pieces (AZ91 and FSPed AZ91). Dry machining was adopted in the present study. Cutting forces were recorded with the help of the dynamometer. The measurements were started as soon as the drill bit touched the work piece surface for a few seconds during the drilling. After drilling, the edges of the holes were analyzed by optical microscope.

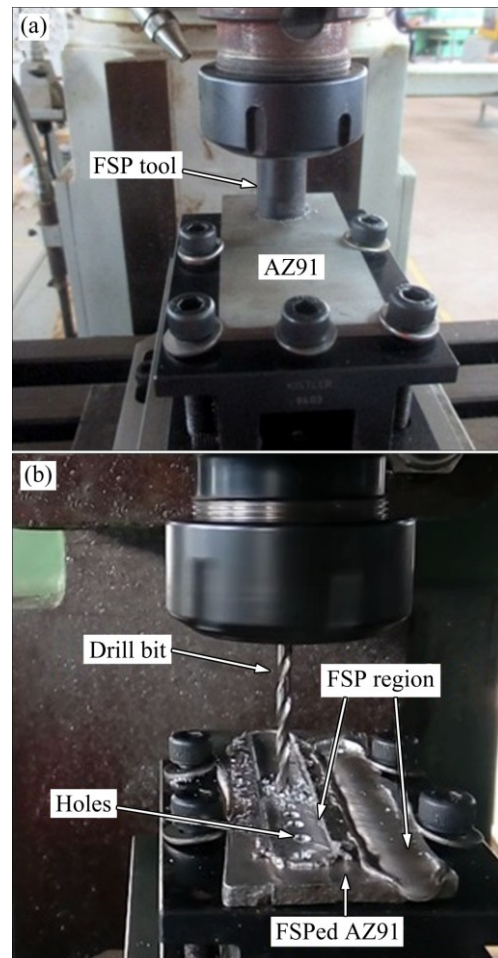


Fig. 1 Photographs obtained during processing: (a) Friction stir processing of AZ91 Mg alloy; (b) Drilling holes on FSPed AZ91 Mg alloy

3 Results and discussion

The normalized XRD patterns of the samples before and after FSP compared in Fig. 2 confirm the starting material as AZ91 Mg alloy. The peaks were identified as α -Mg which is a solid solution of magnesium and aluminium; and β -phase ($Mg_{17}Al_{12}$) which is a compound formed between magnesium and aluminium. The intensities of (100), (101), (102) and (103) peaks were decreased and (002) and (004) peaks were increased after FSP, which is an indication to the resulted preferred orientation due to FSP. Usually, in as-cast condition, (101) peak appears with the highest intensity in Mg. During FSP, the material beneath the shoulder of the FSP tool has undergone severe plastic deformation and the shear along the surface of the work piece [11] produced texture with higher fraction of (002) basal planes as shown in Fig. 2. From the XRD analysis of FSPed AZ91 alloy, the intensities of the peaks corresponding to $Mg_{17}Al_{12}$ were observed as decreased which is an indication to the reduced amount of secondary phase after FSP.

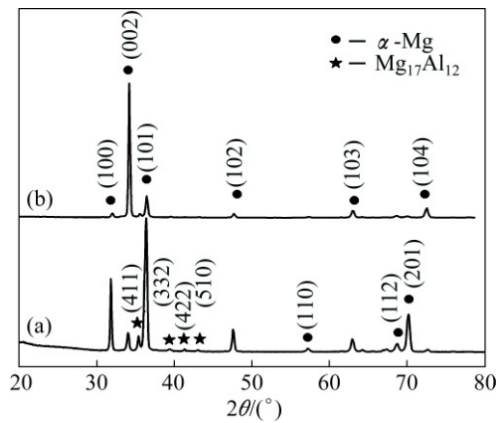


Fig. 2 XRD patterns of AZ91 Mg alloy before (a) and after (b) FSP

Figure 3 shows the optical microscope images obtained in different regions of FSPed AZ91 alloy. The presence of secondary phase (β , $Mg_{17}Al_{12}$) at the grain boundaries as a network like structure can be clearly seen

as indicated by black arrow from Fig. 3(a). Adjacent to the β phase, the presence of the eutectic region ($\alpha+\beta$) can be seen as indicated by the white arrow. In aluminium and zinc (AZ) series Mg alloys, the maximum solubility of aluminium is limited to 1% at the room temperature and forms a solid solution (α) [12]. If the amount of aluminium is increased to more than 1%, a compound of magnesium and aluminium ($Mg_{17}Al_{12}$) is formed which usually appears at α grain boundaries as shown in Fig. 3(a). In the present work, grain refinement was achieved from (166.5 ± 8.7) μm to (21.7 ± 13.5) μm after FSP, as shown in Fig. 3(b). It is also interesting to observe that the β phase is greatly affected as the network-shaped $Mg_{17}Al_{12}$ is invisible from the optical microscope images (Fig. 3) after FSP. This phenomenon can be explained by observing the phase diagram of magnesium and aluminum. The solubility limit of aluminum is increased with respect to the temperature. The maximum solubility of aluminum (12.6%) in magnesium can be seen at 437 °C. In FSP, the

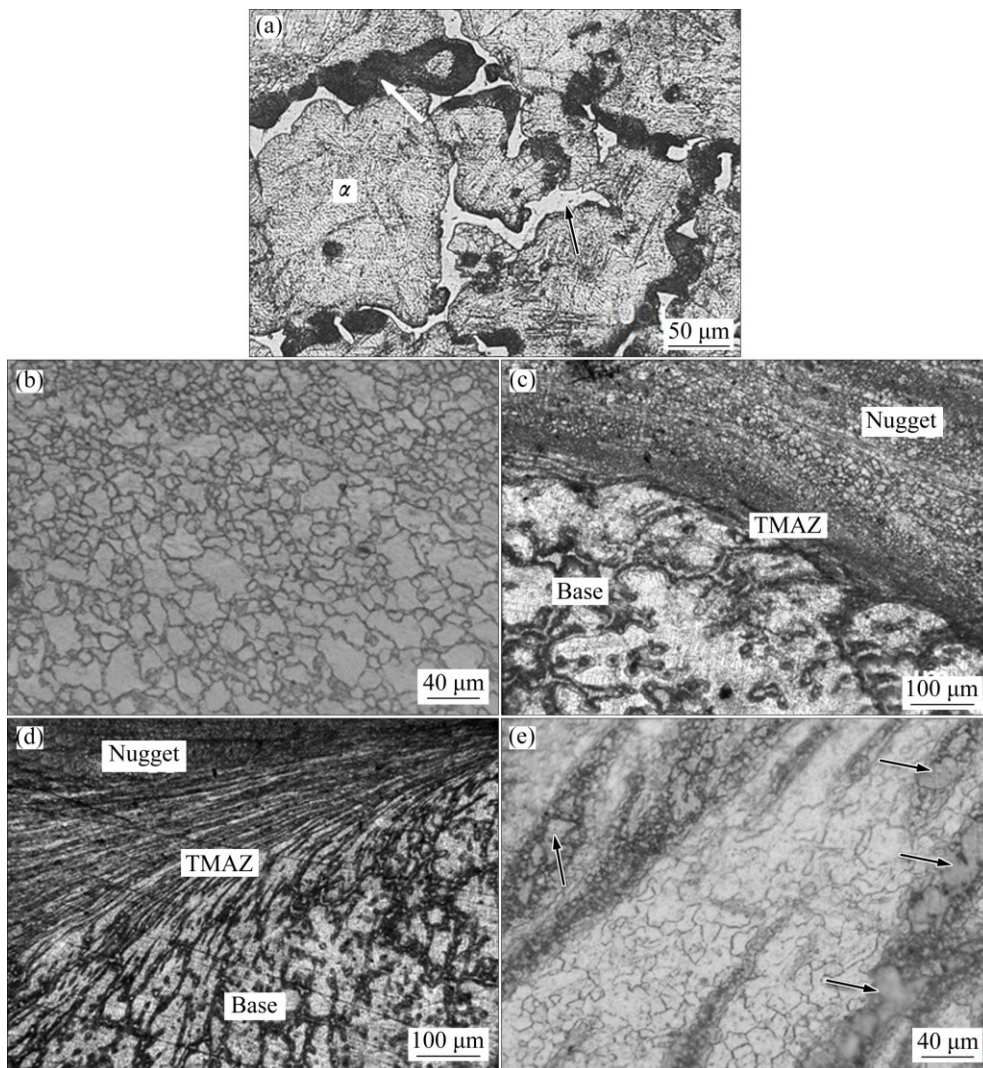


Fig. 3 Optical microscope images of samples: (a) AZ91; (b) Nugget zone of FSPed AZ91; (c) TMAZ at retreating side; (d) TMAZ at advancing side; (e) Magnified image of (d)

temperature in the nugget zone will reach 0.7–0.8 times of base material melting temperature [13,14]. The formation of β phase was suppressed during the dynamic recrystallization and fine α grains were produced in FSPed AZ91. The thermo-mechanical affected zone (TMAZ) at the retreating side (Fig. 3(c)) shows a narrow interface region whereas the TMAZ at the advancing side (Fig. 3(d)) shows a wide region. Interestingly in the TMAZ at the advancing side, the magnified image (Fig. 3(e)) clearly confirms the evolution of smaller grains and reduction of secondary phase as discontinuous small regions indicated with black arrows. Therefore, it can be understood from the microstructural studies and XRD analysis that more amount of β phases were dissolved and produced α grains with rich aluminium (super saturated solid solution grains) after FSP.

Figure 4(a) shows the average hardness of the samples. Surprisingly, the hardness was found to be decreased for FSPed AZ91 (88.95 ± 6.1) compared with AZ91 (104.1 ± 14.6). Figure 4(b) shows the hardness distribution across the FSPed region compared with AZ91. The hardness was observed as decrease within the stir zone compared with the base material. The variations in the measured values were more (maximum HV 129.5 and minimum HV 86.3) for AZ91 compared with the stir zone of FSPed AZ91. The hardness variation in AZ91 can be attributed to the presence of both brittle and hard β -phase/eutectic regions at the α -grain boundaries. During measuring the hardness, if the indent was placed on the β -phase or eutectic region, higher hardness is inevitably recorded as clearly demonstrated in our earlier report [10]. When the indent is placed on any α -grain, the corresponding hardness is lower.

In the present study after FSP, β -phase was suppressed and the α -grains have become super saturated with aluminium. A slight increase was noticed in the hardness (HV 88.95) of FSPed AZ91 compared with the hardness measured at the α -grains of unprocessed AZ91 (HV 86.3). The hardness was expected to be higher after FSP due to grain size reduction and also due to solid solution strengthening. Surprisingly, in the present study, hardness was decreased after FSP. The results demonstrate the prominent effect of $Mg_{17}Al_{12}$ phase on hardness of AZ series Mg alloys. The presence of the β -phase in the form of network-like structure and also in the eutectic regions at the grain boundaries of α -grains as shown in Fig. 3(a) plays an important role in the hardness of AZ91 Mg alloy compared with the grain size reduction effect. Therefore, it can be understood that the role of secondary phase on the hardness is prominent which dominated the grain refinement effect. After FSP, the contribution of grain size to increase the hardness in the stir zone was lower compared with the effect of the loss of the secondary phase distribution on the reduction

of the hardness. Hence, the overall effect brought the average hardness of FSPed AZ91 to a lower value compared with AZ91.

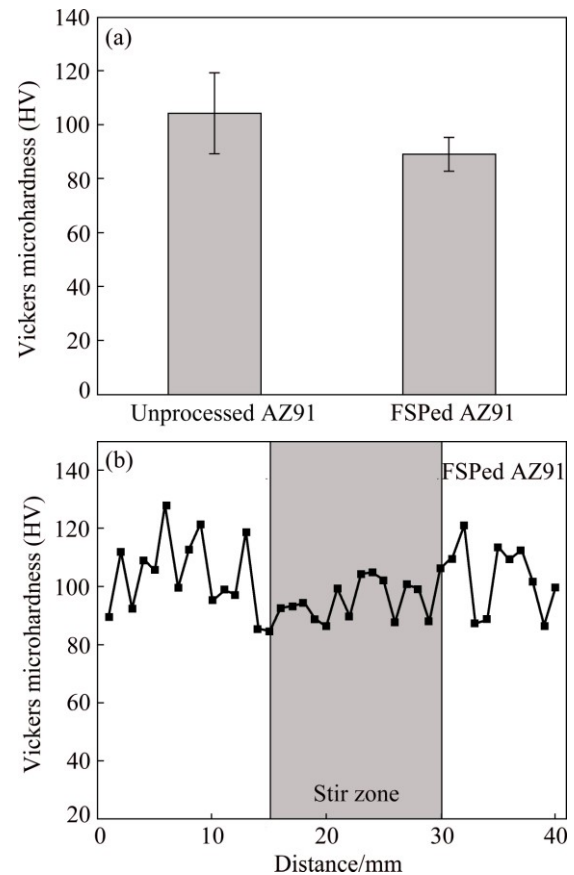


Fig. 4 Hardness measurements of samples: (a) Average hardness; (b) Hardness distribution

Figure 5 shows the cutting force (F_z) profiles of AZ91 and FSPed AZ91 at different machining parameters. It can be clearly seen that the cutting forces were higher for FSPed AZ91 compared with AZ91. It can also be clearly seen that the cutting forces decreased with the increase of cutting speeds as per the theory of metal cutting [10]. As the feed rate was increased from 16 mm/min to 20 mm/min and 25 mm/min, a hike followed by sudden decrease in cutting force was observed. When the drill bit touched the surface of the work piece, cutting force to remove the material was gradually increased until the cutting edges were completely penetrated into the work piece. Then, the relief on the drill bit led to decrease the cutting forces as the hole diameter reached the diameter of the drill bit. The mean cutting forces at different speeds are compared in Fig. 6. The variations within the work piece are also found to be higher. As the speed was increased from 90 to 180 r/min, considerable decrease in the cutting forces can be clearly observed for both AZ91 and FSPed AZ91. However, when the speed was increased from 180 to 355 r/min, the increase in mean cutting force was lower

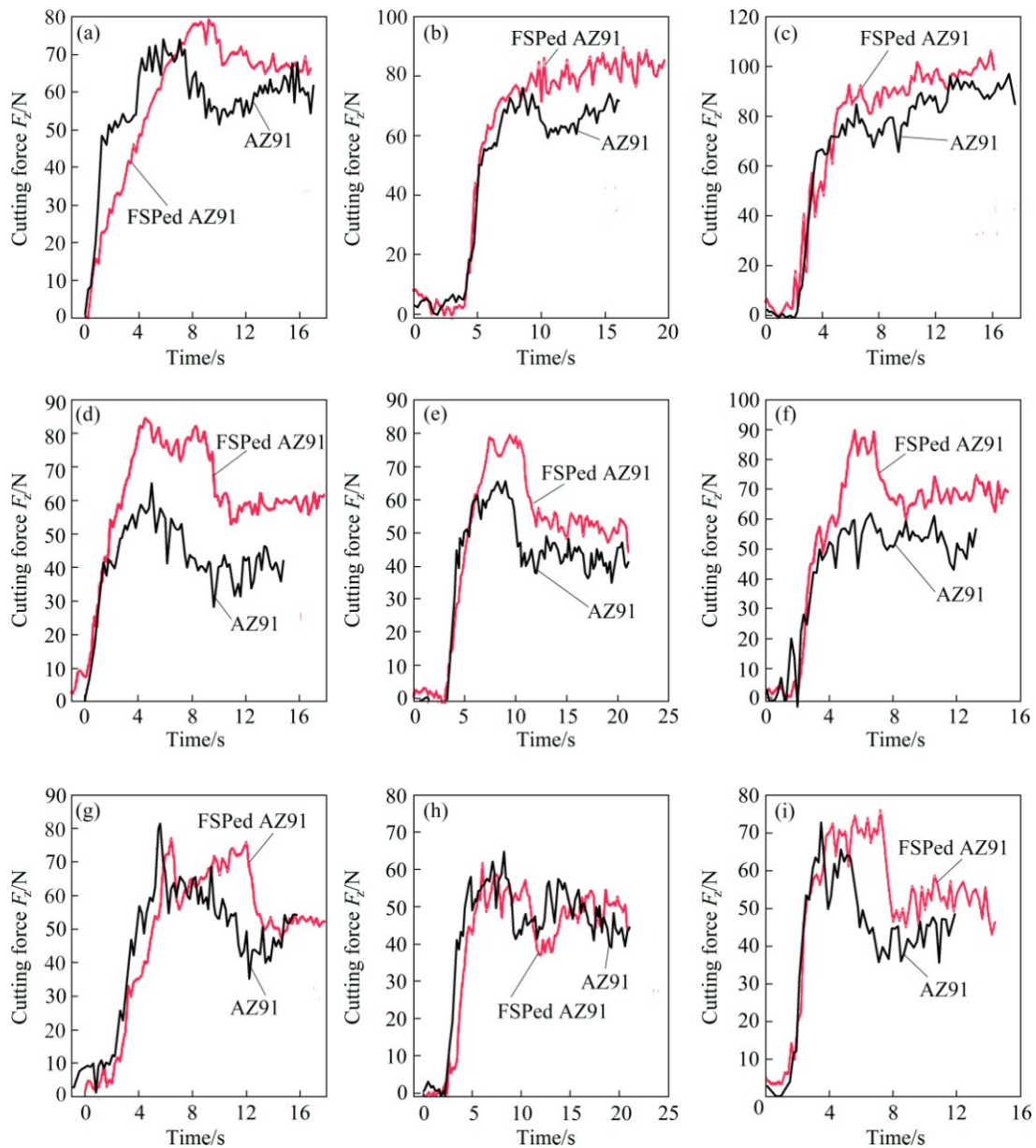


Fig. 5 Cutting force (F_z) profiles recorded during drilling of unprocessed (AZ91) and processed (FSPed AZ91) sheets at different cutting speeds and feeds: (a) 90 r/min and 16 mm/min; (b) 90 r/min and 20 mm/min; (c) 90 r/min and 25 mm/min; (d) 180 r/min and 16 mm/min; (e) 180 r/min and 20 mm/min; (f) 180 r/min and 25 mm/min; (g) 355 r/min and 16 mm/min; (h) 355 r/min and 20 mm/min; (i) 355 r/min and 25 mm/min

for both AZ91 and FSPed AZ91. As the cutting speed was increased during drilling, the corresponding temperature was also increased which reduced the yield strength of the material locally at the vicinity of the hole. Therefore, at higher speeds, the material was plastically deformed in the form of chips at lower cutting forces. From the results it is evident for all the cases that the FSPed AZ91 has higher mean cutting forces compared with AZ91.

The two important mechanisms which played a vital role in increasing the cutting forces in FSPed AZ91 are solid solution strengthening and grain boundary

strengthening. After FSP, more amount of solute (aluminium) was dissolved in the solvent (magnesium) that is the reason why $Mg_{17}Al_{12}$ phase was greatly affected in FSPed AZ91. The average grain size was also reduced after FSP as shown in Fig. 3(b). Therefore, the fine-grained super saturated FSPed AZ91 has more resistance towards the machining during drilling which appeared with increased cutting force compared with AZ91. Figure 7 shows the typical optical microscope images of the edges of holes on AZ91 and FSPed AZ91 drilled at speed of 90 r/min and feed of 16 mm/min. It can be clearly seen the affected edges for both the

samples. More damage was observed for AZ91 compared with FSPed AZ91, as shown in Figs. 7(b) and (d). The same observation was made at all the cutting

speeds and feeds as shown in Fig. 8.

As the cutting speed was increased from 90 r/min to 180 r/min and 355 r/min, the mean effected edge was

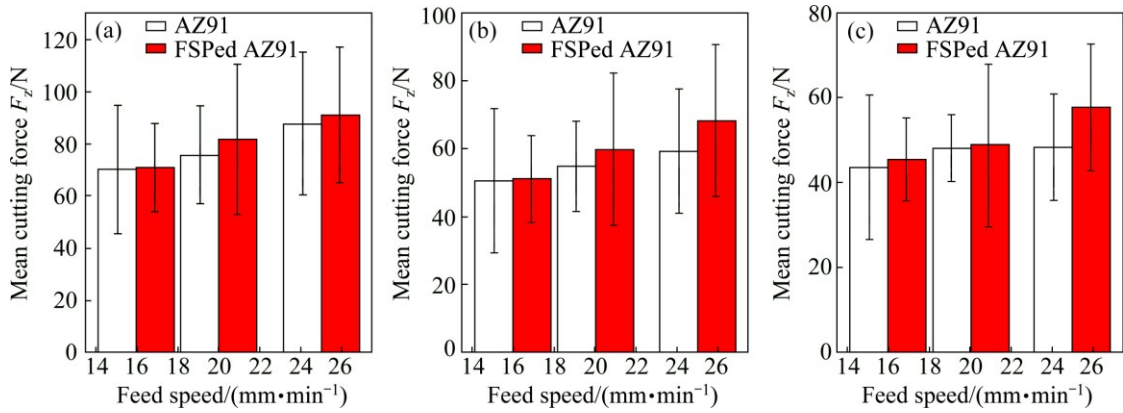


Fig. 6 Comparison of mean cutting forces at different feed speeds: (a) 90 r/min; (b) 180 r/min; (c) 355 r/min

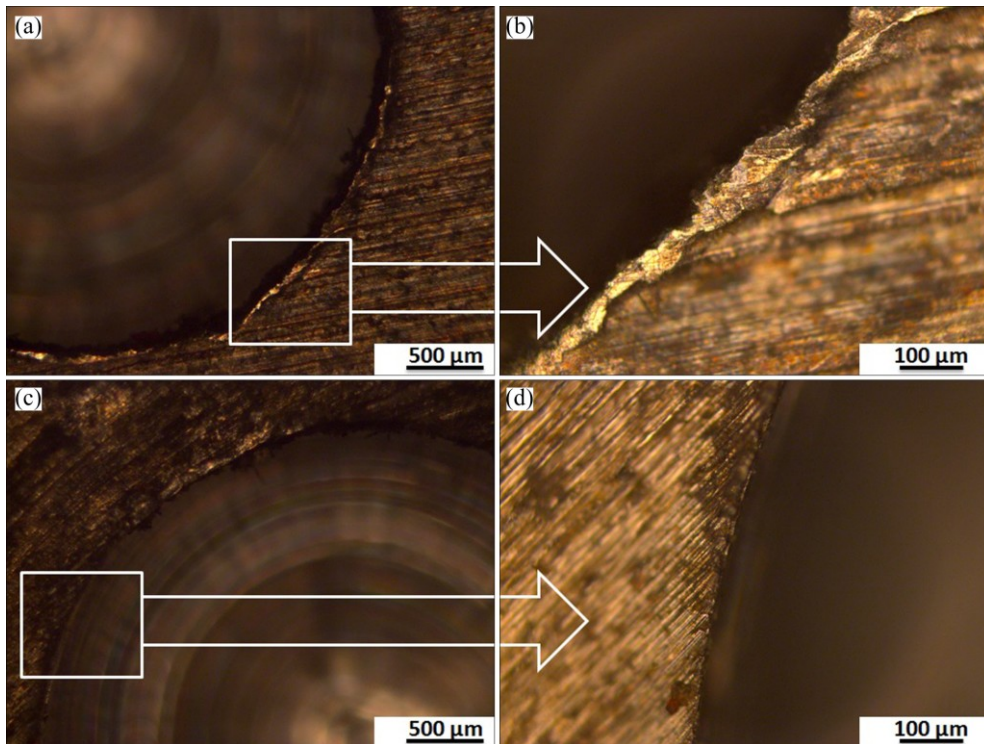


Fig. 7 Typical optical microscope images of drilled hole edge at cutting speed of 90 r/min and feed speed of 16 mm/min: (a) AZ91; (b) Corresponding magnified image of square in (a); (c) FSPed AZ91; (d) Corresponding magnified image of square in (c)

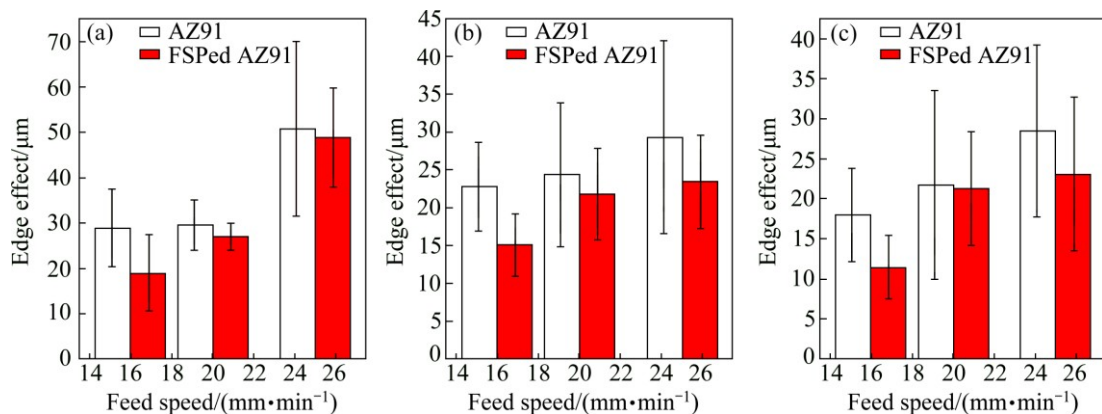


Fig. 8 Edge effect measurements for holes drilled at different cutting speeds: (a) 90 r/min; (b) 180 r/min; (c) 355 r/min

decreased for AZ91 and FSPed AZ91. As it was observed in the analysis of the cutting forces, the localized ductility of the samples was increased due to the generated heat with increase in cutting speed which has a major role in material removal and the edge damage. Additionally, the grain size and the presence of secondary phase also played important role. In the present study, fine-grained FSPed AZ91 showed the holes with less edge effect at higher cutting forces during drilling compared with AZ91. Figure 9 shows the schematic illustration of the drilling of coarse-grained AZ91 and fine-grained FSPed AZ91. Unprocessed AZ91 has coarse grains with good amount of $Mg_{17}Al_{12}$ and FSPed AZ91 has fine grains with insignificant amount of secondary phase. While machining, the coarse grains form longer chips with dip serrations compared with fine grains as explained by LAPOVOK et al [5]. Therefore, as schematically shown in Fig. 9, more grains which may have random orientation and increased fraction of grain boundary which is a mismatch region between the grains come in contact against the cutting edges as the drill bit penetrates into the material are the two important factors which led to increasing the cutting force required to plastically deform the material in the form of chips.

It can be understood from the results by correlating the hardness and cutting forces that, material with lower hardness (FSPed AZ91) has recorded with higher cutting forces compared with the material with higher hardness (AZ91). This phenomenon can be understood by considering the strain rate effect on cutting forces during machining also explained by SUN et al [15], while cutting titanium alloys. It is true that the cutting force is measured during the plastic deformation at high strain rate of the material and hardness (by indentation method)

is measured under static load conditions. During drilling, strain rate influences the cutting forces. For the same set of machining parameters, the response of the material against strain rate is certainly different for FSPed AZ91 compared with AZ91. FSPed AZ91 is expected to exhibit higher resistance to plastic deformation due to strain hardening, which is attributed to the super saturation of magnesium with aluminium. Therefore, even though the hardness was lower for FSPed AZ91, the cutting forces increased compared with AZ91.

The interest on fine grained metals is tremendously growing in the materials research field due to their excellent mechanical properties. However, in order to develop structures using these modern engineered materials, machining is inevitable. Therefore, understanding the machining characteristics of grain refined materials is crucial. In the context of light metals usage for energy efficient applications, machining of magnesium alloys is greatly needed. Hence, the present study demonstrates valuable information on the effect of grain size and secondary phase on machining characteristics during drilling. Based on the results it can be concluded that the friction stir processing can be used as a potential tool to develop fine-grained super saturated AZ91 Mg alloy and the higher cutting forces should be considered while designing machining operations to develop structures using these fine-grained AZ91 Mg alloys. Lower damage introduced to the base material during machining of fine-grained AZ91 Mg alloy compared with AZ91 indicates better machining characteristics with grain refinement and secondary phase reduction. Lower hole damage also extends the life of the structure by reducing failure susceptibility due to lower stress concentrated regions at the edge of the holes.

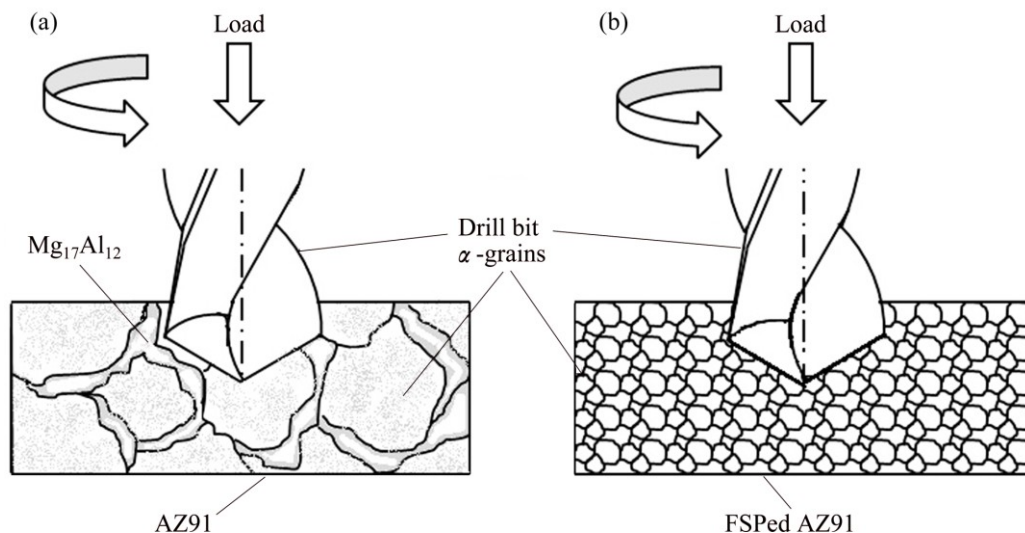


Fig. 9 Schematic representation of drilling in samples: (a) AZ91; (b) FSPed AZ91

4 Conclusions

Friction stir processing was successfully adopted to process AZ91 Mg alloy. Grain refinement from a starting size of $(166.5 \pm 8.7) \mu\text{m}$ to $(21.7 \pm 13.5) \mu\text{m}$ was obtained. The grains were found to be super saturated with negligible secondary phase in the nugget zone. Hardness was found to be decreased after FSP due to the absence of brittle and hard secondary phase in spite of grain refinement. The cutting forces were observed as marginally increased because of the grain refinement and solid solution strengthening. The material removal characteristics were also found to be better for fine-grained FSPed AZ91 as observed in the hole edge damage studies. Hence, from the present study, it can be concluded that the grain refinement by FSP certainly influences the machining characteristics during drilling.

Acknowledgements

The authors would like to thank Mr. Chandrasekhar, Foreman, Mr. Ayub Khan and Mr. Siva Krishna, Laboratory Assistants, Department of Mechanical Engineering, RGUKT Nuzvid, for their help in carrying the present work.

References

- [1] FRIDRICH H E, MORDIKE B L. Magnesium technology [M]. Heidelberg, Germany: Springer, 2006.
- [2] MORDIKE B L, EBERT T. Magnesium properties—applications – potential [J]. Materials Science and Engineering A, 2001, 302: 37–45.
- [3] MISHRA R S, MA Z Y. Friction stir welding and processing [J]. Materials Science and Engineering R, 2005, 50: 1–78.

- [4] PATHAK J P, TIWARI S N. Chip formation in machining of Al–Si alloy [J]. Indian Foundry Journal, 1995, 41(1): 1–8.
- [5] LAPOVOK R, MOLOTNIKOV A, LEVIN Y, BANDARANAYAKE A, ESTRIN Y. Machining of coarse grained and ultra fine grained titanium [J]. Journal of Materials Science, 2012, 47: 4589–4594.
- [6] FRIEMUTH T, WINKLER J. Machining of magnesium work pieces [J]. Advanced Engineering Materials, 1999, 1(3–4): 183–186.
- [7] FANG F Z, LEE L C, LIU X D. Mean flank temperature measurement in high speed dry cutting of magnesium alloy [J]. Journal of Materials Processing Technology, 2005, 167: 119–123.
- [8] ARAI M, SATO S, OGAWA M, SHIKATA H I. Chip control in finish cutting of magnesium alloy [J]. Journal of Materials Processing Technology, 1996, 62: 341–344.
- [9] AKYUZ B. Influence of Al content on machinability of AZ series Mg alloys [J]. Transactions of Nonferrous Metals Society of China, 2013, 23: 2243–2249.
- [10] RATNA SUNIL B, GANESH K V, PAVAN P, VADAPALLI G, SWARNALATHA Ch, SWAPNA P, BINDUKUMAR P, PRADEEP KUMAR REDDY G. Effect of aluminum content on machining characteristics of AZ31 and AZ91 magnesium alloys during drilling [J]. Journal of Magnesium and alloys, 2016, 4: 15–21.
- [11] PARK S, SATO Y, KOKAWA H. Basal plane texture and flow pattern in friction stir weld of a magnesium alloy [J]. Metallurgical and Materials Transactions A, 2003, 34: 987–994.
- [12] AVEDESIAN M M, BAKER H. ASM specialty handbook, magnesium and magnesium alloys [M]. Materials Park, Ohio, USA: ASM International, 1999.
- [13] MISHRA R S, MAHONEY M W, McFADDEN S X, MARA N A, MUKHERJEE A K. High strain rate super plasticity in a friction stir processed 7075 Al alloy [J]. Scripta Materialia, 2000, 42: 163–168.
- [14] AZIZIEH M, KOKABI A H, ABACHI P. Effect of rotational speed and probe profile on microstructure and hardness of AZ31/Al₂O₃ nanocomposites fabricated by friction stir processing [J]. Materials and Design, 2011, 32: 2034–2041.
- [15] SUN S, BRANDT M, DARGUSCH M S. Characteristics of cutting forces and chip formation in machining of titanium alloys [J]. International Journal of Machine Tools & Manufacture, 2009, 49: 561–568.

搅拌摩擦加工细晶 AZ91 镁合金的加工特性

G. V. V. SURYA KIRAN¹, K. HARI KRISHNA¹, Sk. SAMEER¹, M. BHARGAVI¹, B. SANTOSH KUMAR¹, G. MOHANA RAO¹, Y. NAIDUBABU¹, RAVIKUMAR DUMPALA², B. RATNA SUNIL¹

1. Department of Mechanical Engineering,

Rajiv Gandhi University of Knowledge Technologies (AP-IIIT), Nuzvid 521202, India;

2. Department of Mechanical Engineering, Visvesvaraya National Institute of Technology, Nagpur 440010, India

摘要: 搅拌摩擦加工细化 AZ91 镁合金, 研究钻孔过程中不同切割速度和进料速率下晶粒尺寸和二次相对加工特性的影响。经搅拌摩擦加工得到了过饱和 AZ91 镁合金, 晶粒尺寸由 $(166.5 \pm 8.7) \mu\text{m}$ 细化到 $(21.7 \pm 13.5) \mu\text{m}$ 。相比未加工的 AZ91 镁合金 (HV(108.2±15.6)), 经搅拌摩擦加工的合金硬度为 HV(88.95±6.1), 这归因于二次相的减少。然而, 搅拌摩擦加工 AZ91 合金的平均切割力略微减小。相比未加工的 AZ91 镁合金, 搅拌摩擦加工 AZ91 合金的钻孔边缘损伤较低。因此, 虽然在钻孔过程中晶粒细化可以略微增大切割力, 但在 AZ91 镁合金加工过程中边缘处理较好。

关键词: 镁合金; 搅拌摩擦加工; 机械加工; 晶粒尺寸; 显微组织